Control of oxygen sublattice structure in ultra-thin SrCuO2 films studied by X-ray photoelectron diffraction

Bouwe Kuiper, D. Samal, Dave H. A. Blank, Johan E. ten Elshof, Guus Rijnders, and Gertjan Koster

Citation: APL Materials **1**, 042113 (2013); doi: 10.1063/1.4824779
View online: http://dx.doi.org/10.1063/1.4824779
View Table of Contents: http://scitation.aip.org/content/aip/journal/aplmater/1/4?ver=pdfcov
Published by the AIP Publishing

APL MATERIALS **1**, 042113 (2013)

Control of oxygen sublattice structure in ultra-thin $SrCuO_2$ films studied by X-ray photoelectron diffraction

Bouwe Kuiper, D. Samal, Dave H. A. Blank, Johan E. ten Elshof, Guus Rijnders, and Gertjan Koster[a]

Faculty of Science and Technology and MESA+ Institute for Nanotechnology, University of Twente, Post Office Box 217, 7500 AE Enschede, The Netherlands

(Received 2 August 2013; accepted 27 September 2013; published online 11 October 2013)

Epitaxial and atomically smooth ultra-thin $SrCuO_2$ films are grown on $SrTiO_3$ substrates using pulsed laser deposition. The structural and chemical aspects of these single-layer films of various thickness are characterized using *in situ* X-ray photoelectron diffraction (XPD) and photoelectron spectroscopy. By comparing XPD scans to multiple-scattering electron diffraction simulations, we demonstrate a structural transformation from bulk-planar to chain-type $SrCuO_2$ as the film thickness is reduced from 9 to 3 unit-cells. This observation is in agreement with the recent theoretical prediction [Z. Zhong, G. Koster, and P. J. Kelly, Phys. Rev. B **85**, 121411(R) (2012)] and opens new pathways for structural tuning in ultra-thin films of polar cuprates. [http://dx.doi.org/10.1063/1.4824779]

In recent years there has been a dramatic increase in designing, growing, and characterizing novel complex oxide materials with atomic precision that give rise to greater functionality. The study of the resulting atomically engineered layers and interfaces has proven to be a promising field of research, with the opportunity to manipulate and control various degrees of freedom, e.g., electronic, lattice, spin, and orbital at the atomic scale. Specifically, for the case of ABO_3 complex oxide thin films, the shape, rotations, and distortions of the BO_6 oxygen octahedral due to epitaxial strain and/or lattice defects play a crucial role in the resulting physical properties.[1,2] Moreover, the structure of the oxygen sublattice at the interface between polar and non-polar materials, e.g., $LaAlO_3$- $SrTiO_3$[3] plays a vital role in many of the exotic interfacial phenomena. Therefore, the local structure at interfaces and in ultra-thin layers is of great importance in such systems and needs to be explored precisely.

The infinite layer tetragonal $SrCuO_2$ ($a = b = 3.926$ Å, $c = 3.432$ Å)[4] is one of the parent structures in the cuprate family that hosts high T_C superconductivity.[5–7] Its structure can be considered as an oxygen deficient perovskite, where one oxygen atom is missing in the Sr^{2+} plane. Essentially, its structure is planar and can be viewed as an alternative stacking of Sr^{2+} and CuO_2^{2-} planes;[8] where each Cu^{2+} ion is four-fold coordinated to O^{2-} ions forming CuO_4 plaquettes. Since each alternative constituent atomic plane has a formal charge of $+/-2e$; it leads to a built-in electrostatic potential, which increases with the $SrCuO_2$ thickness.[8]

The recent study by Zhong *et al.*[9] on ultra-thin films of $SrCuO_2$ predicts a structural transformation from bulk planar to a chain-type structure upon reducing the thickness below ~5 unit-cells, that relieves the built-in internal electrostatic potential in $SrCuO_2$. Effectively this phase transformation is caused by an atomic reconstruction, where one oxygen atom is moved from the CuO_2^{2-} plane to the Sr^{2+} plane; thereby making the charge neutral SrO and CuO atomic planes. The modified chain-type structure can be viewed as if the CuO_4 plaquettes are stacked along a perpendicular direction as

[a]Electronic mail: g.koster@utwente.nl

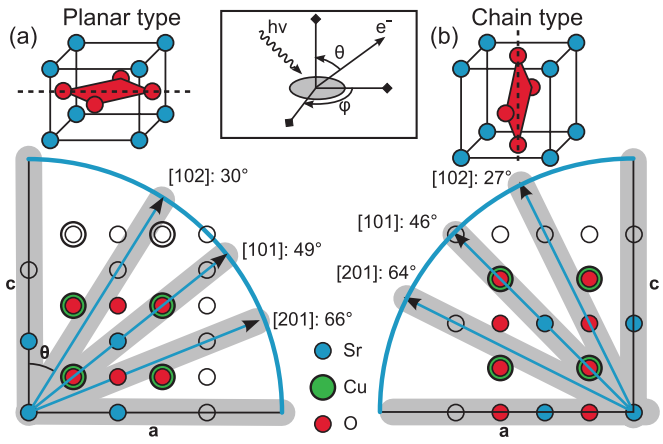

FIG. 1. Schematic drawing of the crystal structure of (a) planar or infinite layer $SrCuO_2$ and (b) chain-type $SrCuO_2$. Strong forward scattering angles [101], [102], and [201] are shown for both structures and corresponding θ angles are calculated. The central inset schematically indicates the XPD measurement geometry.

compared to that in the case of planar one. A schematic of chain vs plane-type $SrCuO_2$ layering is shown in Figure 1. In the process of rearrangement of oxygen ions, the c-axis lattice parameter of the chain-type $SrCuO_2$ on $SrTiO_3$ is predicted to be increased by 0.5 Å as compared to the bulk-planar counterpart. In fact the recent study by Samal *et al.*[10] demonstrated this effect, which clearly shows a change in the oxygen sublattice as a function of $SrCuO_2$ thickness in $SrCuO_2$-$SrTiO_3$ superlattice heterostructures. In addition, the work by Aruta *et al.*[11] on $CaCuO_2$-$SrTiO_3$ superlattice heterostructures also hypothesized the possible formation of CuO chain-type layering at the interface that in a way relieves the built-in electrostatic potential in $CaCuO_2$. Realization of artificially made chain-type structures in ultra-thin $SrCuO_2$ layers will open new routes to design/engineer novel superconducting cuprate-hybrids, with alternation of chain and plane-type structures (the basic structural paradigm in cuprates) that can give more insight into the study of high Tc cuprates at a fundamental level. Moreover, a recent study suggests that the addition of a $SrCuO_2$ epilayer strongly reduces the impurity scattering at the conducting interfaces in oxide $LaAlO_3$-$SrTiO_3$ heterostructures, opening the door to higher carrier mobility materials.[12]

Despite a great deal of interest in infinite layer ultra-thin polar cuprate films, no studies on the structure of bare/single layer ultra-thin films are found in the literature. Ultra-thin single-layer films should be much cleaner to study as compared to superlattice heterostructures made out of the same layers. In the case of superlattice heterostructures more complexity arises due to the addition of many interfaces that lead to chemical intermixing, interdiffusion, roughening, etc. We here study such bare thin films of $SrCuO_2$.

Oxygen atomic positions in such materials can be studied using various techniques, e.g., by measuring the oxygen positions and tilt patterns using X-ray diffraction[1,2] or by using transmission electron microscopy.[13] Alternatively it is possible to probe the local structure using electron diffraction[14] or X-ray photoelectron diffraction (XPD).[15–17] In particular, the latter technique, XPD, is highly suitable to study ultra-thin films, due to its high surface sensitivity and element specific structural information. Moreover, it does not require any sample preparation, it can be applied to films with less than one full layer of coverage and it is a non-destructive method. XPD has been successfully applied to various oxide thin film systems, which provides unique information about the oxygen displacement, even with displacements of a fraction of an angstrom.[16] For example, XPD has been used to analyze the surface structure of $SrTiO_3$[15,18] by comparison of experimental data with multiple scattering simulations. Here, we use this technique to study the novel structural transformation in ultra-thin polar infinite-layer $SrCuO_2$.

We provide here the results of a detailed structural study on bare $SrCuO_2$ layers in the ultra-thin limit, that essentially supports the prediction[9] for a structural transformation from planar to chain-type with reducing $SrCuO_2$ thickness. By using XPD we have been able to measure the

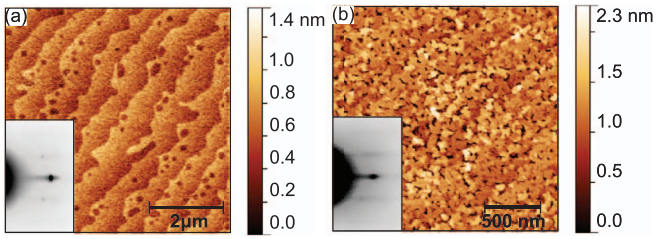

FIG. 2. AFM micrographs of (a) 3 unit-cells of $SrCuO_2$ on $SrTiO_3$ and (b) 9 unit-cells of $SrCuO_2$. Insets show the corresponding RHEED patterns after growth of $SrCuO_2$. Slight surface roughening is observed in the 9 unit-cell film.

precise change in the c-axis lattice parameter between the chain and plane-type $SrCuO_2$ layers. Multiple-scattering electron diffraction calculations based on the program EDAC[19] are used to simulate diffraction patterns that match the experimental data. A similar approach was used on a related cuprate, CuO, in ultra-thin form, to successfully detect a tetragonal phase.[20] Moreover, X-ray photoelectron spectroscopy (XPS) is used to quantitatively compare the film stoichiometry and account for the possible change in electronic structure between chain-type and planar $SrCuO_2$.

Samples are grown by pulsed laser deposition using a Twente Solid State Technology BV system with a laser fluence of 2.0 J/cm^2, a spotsize of 1.8 mm^2, laser repetition rate of 1 Hz, substrate temperature of 650 °C, target substrate distance of 5 cm, and a pressure of 0.3 mbar oxygen. The $SrCuO_2$ target used is oxygen rich, $SrCuO_{2.5}$. Atomic force microscopy (AFM) micrographs are recorded using a Bruker Icon Dimension AFM, in Tapping Mode. XPS and XPD are performed *in situ* on an Omicron nanotechnology GmbH XPS system, with a background pressure of 5×10^{-11} mbar. Measurements were done using a monochromatic Al kα x-ray source, XM1000, and analyzed using a 7 channel EA 125 electron analyzer operated in CAE mode. For the XPD experiments, the acceptance angle of the detector is set to 4°. A Shirley background is subtracted from the XPS spectra, while a linear background is used for XPD spectra. A Thermionics 5 axis sample stage is used for rotating the sample for XPD measurements. Multiple scattering electron diffraction simulations are done using EDAC with a cluster size of ∼700 atoms, a mean free path of 2.3 nm and using 10 iteration steps.

To investigate the predicted structural transition,[9] samples of 3 and 9 unit-cells of $SrCuO_2$ are deposited on TiO_2 terminated[21] 0.05 wt.% Nb doped $SrTiO_3$ substrates. AFM images shown in Figure 2 have rms roughness values of 0.18 and 0.36 nm for 3 and 9 unit-cell films respectively, which is less than the c-axis parameter of $SrCuO_2$, indicating atomically smooth surfaces. The film growth is monitored using *in situ* reflection high energy electron diffraction (RHEED). The RHEED oscillations of the specular reflection are used to determine the growth speed. Both RHEED patterns shown in the insets of Figure 2 are indicative of a two-dimensional/flat surface structure. However, a comparatively weaker intensity of the RHEED pattern corresponding to the 9 unit-cell sample is attributed to increased roughness.

XPD involves the study of electron diffraction patterns recorded using x-ray generated photoelectrons at kinetic energies above 500 eV. At such emission energies, forward scattering effects dominate, which occur along atomic rows. This allows for direct analysis of the crystal structure, since the main peak position can be calculated based on these atomic rows. If for a simple cubic structure the forward scattering along the [001] direction is set at $\theta = 0°$(out-of-plane): the [101] peak occurs at 45°and the [111] at 54°. In the case of $SrCuO_2$ the chain-type structure (c-axis ∼3.8 Å) has a main [101] peak at $\theta = 46°$ ($\tan\theta = 3.9/3.8$) and a planar structure (c-axis ∼3.4 Å) at $\theta = 49°$ ($\tan\theta = 3.9/3.4$). A more detailed picture of these main peaks is given in Figure 1, where the atomic rows of Sr atoms are highlighted with the matching θ angles for both planar and chain-type $SrCuO_2$.

High resolution XPD θ-scans of both $SrCuO_2$ films are depicted in Figure 3 for Cu 2p, Sr 3d, and O 1s electrons. The peak at zero degrees (not shown) is used to correct for sample alignment errors due to deviations in gluing the sample to the sample holder. A clear shift in θ peak positions in the O 1s and Sr 3d scans are observed when compared between 3 unit-cells and 9 unit-cells $SrCuO_2$ films. For clarity, the peak positions are indicated by vertical lines. An overview of all measured peak

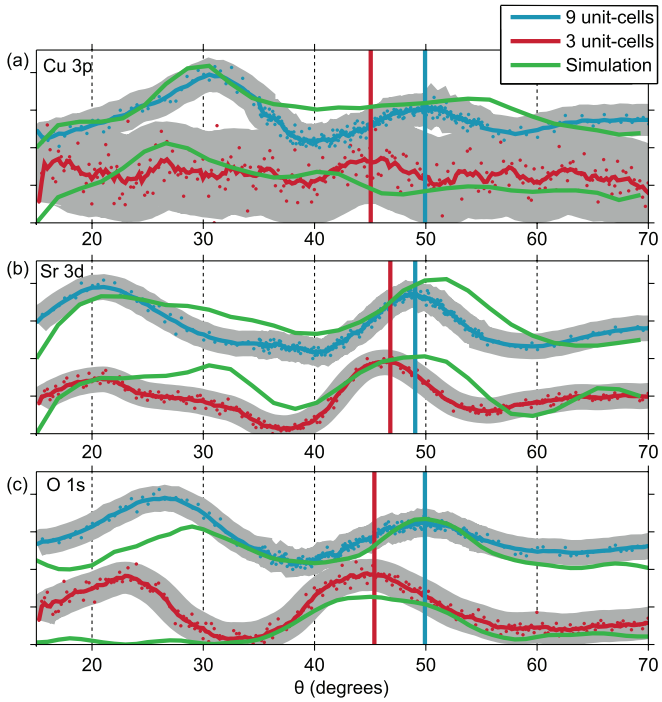

FIG. 3. XPD measurements and simulations of $SrCuO_2$ ulta-thin films of 3 and 9 unit-cells in thickness. θ scans are shown for (a) Cu 3p, (b) Sr 3d, and (c) O 1s. The dots are measured data points, similar colored solid lines are acquired by applying a 9 point moving average. EDAC simulation results are shown in green.

TABLE I. XPD peak positions and corresponding c-axis lengths based on a forward scattering approximation on the left. Right side indicates XPS relative intensities for Sr 3d, Cu 2p, O 1s, and Ti 2p high resolution spectra. A 20%, 20%, 60% distribution is expected for stoichiometric $SrTiO_3$ and 25%, 25%, 50% for $SrCuO_2$. A Shirley background is removed and relative sensitivity factors[24] are taken into account. The substrate contributions to the spectral weight of Sr and O are removed by assuming a stoichiometric contribution of $SrTiO_3$ based on the Ti peak. Relative intensities without this correction are shown in brackets.

	θ peak position and c-axis			Relative XPS intensity (±5%)			
	Sr 3d	Cu 3p/Ti 2p	O 1s	Sr 3d	Cu 2p	O 1s	Ti 2p
3 unit-cells	46.8°± 1°	45.0°± 1°	45.4°± 1°	30%	23%	47%	0%
$SrCuO_2$	3.7 ± 0.1 Å	3.9 ± 0.1 Å	3.8 ± 0.1 Å	(24%)	(11%)	(54%)	(11%)
9 unit-cells	49.0°± 1°	49.9°± 1°	49.9°± 1°	27%	25%	48%	0%
$SrCuO_2$	3.4 ± 0.1 Å	3.3 ± 0.1 Å	3.3 ± 0.1 Å	(26%)	(20%)	(50%)	(4%)
$SrTiO_3$	46°± 1°	45°± 1°	45°± 1°	25%	0%	58%	18%

position is given in Table I, where an average θ shift of ∼3° is observed when increasing the film thickness from 3 to 9 unit-cells. This is in accordance with the expected structural transformation. The contribution from the substrate to the XPD signal is limited by the inelastic mean free path and is most pronounced at low θ angles (normal emission). Based on XPS analysis done below, we estimate a maximum contribution of 11% for normal emission. Therefore, the XPD signal measured between 40° and 50° is not significantly affected by the substrate.

Moreover, the experimental patterns are compared to multiple scattering simulations (green lines) based on the theoretical structures as shown in Figure 1. The Sr 3d scan shows a good agreement between experiment and simulation, both in the peak position and the peak shapes for planar and chain-type structures. The O 1s simulation shows the main peak position at nearly the same value of θ as observed in the experimental data. However, at lower angles the simulations deviate from the experimental data for the chain-type structure. The Cu 3p simulations do not show

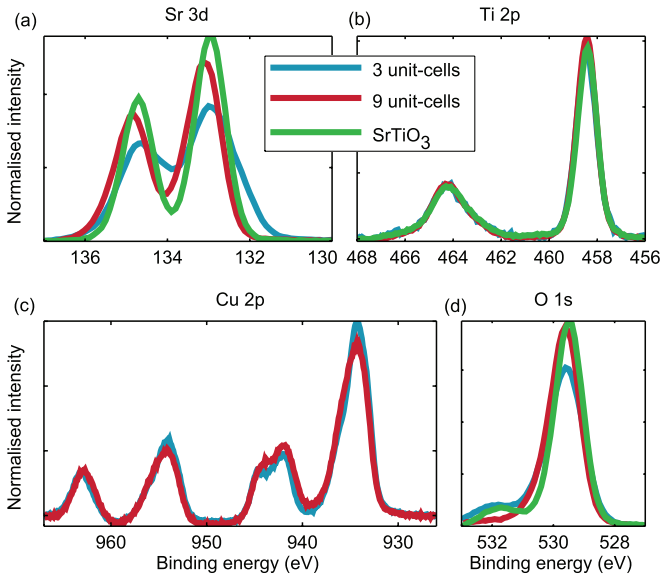

FIG. 4. Photoelectron spectra of $SrCuO_2$ core levels of (a) Sr 3d, (b) Ti 2p, (c) Cu 2p, and (d) O 1s. For all scans, a Shirley background is subtracted and the intensity normalized to the total area, the Ti 2p spectra are correct for binding energy shifts due to sample charging.

good agreement with the experimental results, but the main experimental peak positions are still in good agreement with the forward scattering mechanism. Moreover, the rather flat and featureless experimental spectrum for the 3 unit-cell sample is at least qualitatively predicted by theory. Small deviations at low θ angles between simulations and experiments might be caused by effects of the substrate on the XPD signal, which is not taken into account in the simulations.

Photoelectron spectra of both $SrCuO_2$ films recorded at normal emission angle ($\theta = 0^\circ$) are shown in Figure 4. Core level spectra of Cu 2p, O 1s, Sr 3d, and Ti 2p of the substrate are plotted. The Ti 2p signal from the $SrTiO_3$ substrate is used to correct the measured binding energies for sample charging effects. For all individual scans a Shirley background is subtracted and the intensity normalized to the total area, in order to compare peak shapes. A Ti 2p signal from the substrate is present in both films. Thus, the observed Sr 3d and O 1s spectral lines contain electrons from both the $SrCuO_2$ film and the $SrTiO_3$ substrate. Small changes in peak shapes of O 1s and Sr 3d are possibly caused by these substrate contributions. Moreover, in the O 1s spectrum, near 532 eV, a low intensity peak related to surface contaminants is observed in all films. A subtle change is observed in the Cu 2p spectrum near the main peak at 937 eV, as well as in the structure near 942 eV. These changes are possibly caused by a change in coordination number or bond distance.[20,22,23] However, these are hard to quantify and beyond the scope of this work. The observed Cu 2p spectral shape with strong satellites on $2p_{3/2}$ and $2p_{1/2}$ at 943 eV and 963 eV, respectively, indicates a dominant Cu^{2+} valence state in both of our $SrCuO_2$ films.

Quantitative XPS analysis results are given in Table I. The percentages are calculated using calculated Scofield photoelectric cross-sections[24,25] for the relative sensitivity factors. Although the Scofield cross-sections do not take into account machine specific corrections, they yield reasonable results for a $SrTiO_3$ substrate, also given in Table I. In brackets the measured observed relative intensities of Sr 3d, Cu 2p, Ti 2p, and O 1s are given. A Ti 2p signal of different magnitudes is clearly observed for both 3 and 9 unit-cell $SrCuO_2$ films, with this being due to the greater inelastic attenuation of the $SrTiO_3$ signal by the thicker film. Thus, the relative intensities of Sr, Cu, and O will represent a combination of the $SrCuO_2$ film and the underlying $SrTiO_3$ substrate. Therefore, a correction is applied, whereby the observed Ti signal is subtracted from the Sr and O signals, assuming a stoichiometric $SrTiO_3$ contribution. The resulting $SrCuO_2$ compositions are shown without brackets in Table I. This correction assumes a homogeneous $SrCuO_2$ film and no dependence of the kinetic energy for the mean free path of the escaping electrons. The later

assumption increases the experimental error, estimated at around 5%. Taking into account the data analysis methodology, the two $SrCuO_2$ films have a similar stoichiometry within the experimental error.

In summary, a structural phase transition in $SrCuO_2$ ultra-thin films as a function of film thickness is demonstrated using XPD. A film of 3 unit-cells thick is confirmed to be of the chain-type and a 9 unit-cells thick films is of the planar type. Using both simple forward focusing arguments and multiple scattering simulations, the measured peak positions are found to be in accordance with the predicted structure. The observed structural change occurs, while the stoichiometry is conserved, as observed by photoelectron spectroscopy. The present findings provide new insight for designing novel artificial cuprate heterostructures with new electronic properties.

This work was financially supported by the chemical sciences division of the Netherlands Organization for Scientific Research (NWO-CW). D.S. thanks the financial support from AFOSR and EOARD project (Project No. FA8655-10-1-3077). All authors would like to thank Zhicheng Zhong and Michelle Kruize for valuable discussion.

[1] A. Vailionis, H. Boschker, W. Siemons, E. P. Houwman, D. H. A. Blank, G. Rijnders, and G. Koster, Phys. Rev. B **83**, 064101 (2011).
[2] S. J. May, J.-W. Kim, J. M. Rondinelli, E. Karapetrova, N. A. Spaldin, A. Bhattacharya, and P. J. Ryan, Phys. Rev. B **82**, 014110 (2010).
[3] A. Ohtomo and H. Y. Hwang, Nature (London) **427**, 423 (2004).
[4] M. Takano, Y. Takeda, H. Okada, M. Miyamoto, and T. Kusaka, Physica C **159**, 375 (1989).
[5] G. Er, S. Kikkawa, Y. Miyamoto, S. Tanaka, M. Sera, M. Sato, Z. Hiroi, M. Takano, and Y. Bando, Physica C **196**, 271 (1992).
[6] M. Azuma, Z. Hiroi, M. Takano, Y. Bando, and Y. Takeda, Nature (London) **356**, 775 (1992).
[7] M. G. Smith, A. Manthiram, J. Zhou, J. B. Goodenough, and J. T. Markert, Nature (London) **351**, 549 (1991).
[8] G. Koster, A. Brinkman, H. Hilgenkamp, A. J. H. M. Rijnders, and D. H. A. Blank, J. Phys.: Condens. Matter **20**, 264007 (2008).
[9] Z. Zhong, G. Koster, and P. J. Kelly, Phys. Rev. B **85**, 121411(R) (2012).
[10] D. Samal, T. Haiyan, H. Molegraaf, B. Kuiper, W. Siemons, S. Bals, J. Verbeeck, G. Van Tendeloo, Y. Takamura, E. Arenholz, C. A. Jenkins, G. Rijnders, and G. Koster, Phys. Rev. Lett. **111**, 096102 (2013).
[11] C. Aruta, C. Schlueter, T.-L. Lee, D. Di Castro, D. Innocenti, A. Tebano, J. Zegenhagen, and G. Balestrino, Phys. Rev. B **87**, 155145 (2013).
[12] M. Huijben, G. Koster, M. K. Kruize, S. Wenderich, J. Verbeeck, S. Bals, E. Slooten, B. Shi, H. J. A. Molegraaf, J. E. Kleibeuker, S. van Aert, J. B. Goedkoop, A. Brinkman, D. H. A. Blank, M. S. Golden, G. van Tendeloo, H. Hilgenkamp, and G. Rijnders, "Defect engineering in oxide heterostructures by enhanced oxygen surface exchange." Adv. Funct. Mater. (published online).
[13] C. L. Jia, S. B. Mi, M. Faley, U. Poppe, J. Schubert, and K. Urban, Phys. Rev. B **79**, 081405 (2009).
[14] D. I. Woodward and I. M. Reaney, Acta. Crystallogr. **61**, 387 (2005).
[15] A. Pancotti, N. Barrett, L. F. Zagonel, and G. M. Vanacore, J. Appl. Phys. **106**, 034104 (2009).
[16] L. Despont, C. Koitzsch, F. Clerc, M. G. Garnier, P. Aebi, C. Lichtensteiger, J.-M. Triscone, F. J. Garcia de Abajo, E. Bousquet, and P. Ghosez, Phys. Rev. B **73**, 094110 (2006).
[17] D. P. Woodruff, J. Electron Spectrosc. **178–179**, 186 (2010).
[18] J. Kawai, K. Tamura, M. Owari, and Y. Nihei, J. Electron. Spectrosc. **61**, 103 (1992).
[19] F. J. García de Abajo, M. A. Van Hove, and C. S. Fadley, Phys. Rev. B **63**, 075404 (2001).
[20] W. Siemons, G. Koster, D. H. A. Blank, R. H. Hammond, T. H. Geballe, and M. R. Beasley, Phys. Rev. B **79**, 195122 (2009).
[21] G. Koster, B. L. Kropman, G. J. H. M. Rijnders, D. H. A. Blank, and H. Rogalla, Appl. Phys. Lett. **73**, 2920 (1998).
[22] F. Parmigiani, L. E. Depero, T. Minerva, and J. B. Torrance, J. Electron Spectrosc. **58**, 315 (1992).
[23] M. A. van Veenendaal and G. A. Sawatzky, Phys. Rev. Lett. **70**, 2459 (1993).
[24] Quantitative XPS analysis was done using theoretical cross-sections, without taking into account the energy dependent inelastic losses and assuming a homogeneous film. This method allows us to compare the changes in the stoichiometry of $SrCuO_2$ films with respect to each other. However, a more accurate estimation requires the consideration of inelastic losses.
[25] J. H. Scofield, J. Electron Spectrosc. **8**, 129 (1976).